Agricultural and Forest Meteorology 160 (2012) 60–68

Contents lists available at SciVerse ScienceDirect

Agricultural and Forest Meteorology

journal homepage: www.elsevier.com/locate/agrformet

Seasonal patterns of foliar reflectance in relation to photosynthetic capacity and color index in two co-occurring tree species, *Quercus rubra* and *Betula papyrifera*

Sophie Y. Dillen[a,b,*], Maarten Op de Beeck[b], Koen Hufkens[a,c], Michele Buonanduci[a], Nathan G. Phillips[a]

[a] Boston University, Department of Geography and Environment, 675 Commonwealth Avenue, Boston, MA 02215, USA
[b] University of Antwerp, Biology Department, Research Group Plant and Vegetation Ecology, Universiteitsplein 1, 2610 Wilrijk, Belgium
[c] Ghent University, Faculty of Bioscience Engineering, Laboratory of Applied Physical Chemistry, Coupure 653, 9000 Ghent, Belgium

ARTICLE INFO

Article history:
Received 5 October 2011
Received in revised form 4 January 2012
Accepted 4 March 2012

Keywords:
A_n–C_i curve
Digital imaging
Hyperspectral imaging
Maximum rate of carboxylation (V_{cmax})
Maximum rate of electron transport (J_{max})
Nitrogen
Paper birch
Phenology
Red oak
Spectral vegetation index

ABSTRACT

Although foliar reflectance in the visible wavelengths is largely understood, species-specific relations between leaf spectral properties, pigment content and carbon exchange, and interdependence of these fundamental drivers that ultimately produce large-scale signals complicate understanding of and upscaling in remote sensing applications. We recorded seasonal patterns in foliar reflectance in relation to leaf photosynthetic, biochemical, structural and optical properties in two co-occurring tree species, red oak (*Quercus rubra*) and paper birch (*Betula papyrifera*). Over the course of a growing season, we monitored the timing of phenological events, i.e. bud break, near-complete leaf expansion and leaf fall, on mature trees. On a monthly basis, maximum rate of carboxylation (V_{cmax}) and maximum rate of electron transport (J_{max}) were estimated from leaf-level gas exchange measurements in the upper crown for three individuals per species. Thereafter, visible and near infrared spectral properties, nitrogen content and specific leaf area were determined for sampled sunlit leaves. These data were compared with color indices extracted from digital images of sampled leaves throughout the growing season.

Studied leaf traits significantly varied between the two species and throughout the growing season. Paper birch was characterized by relatively early bud break and rapid leaf expansion. Hence, interactions between species and day of year could be partly contributed to contrasting spring phenology of paper birch and red oak. Spectral vegetation indices, Chlorophyll Normalized Difference Index (Chl NDI), Photochemical Reflectance Index (PRI) and in particular Red Edge Position (λRE), gave a good indication of leaf physiology over the course of the growing season, more specifically of photosynthesis and leaf nitrogen on an area basis (N_{area}). On the other hand, color indices performed rather poorly at tracking key leaf functional traits in this study. Overall, dark green leaves characterized by low Intensity (*I*, derived from HSI color space) displayed highest photosynthetic activity and highest values of spectral vegetation indices.

1. Introduction

Forest functioning is principally driven by the biochemical and structural properties of its foliage and seasonal variation therein (Pallardy and Kozlowski, 2008). For decades, remotely sensed information about essential canopy and leaf properties has been obtained through hyper-, multispectral and digital imaging at different scales in space and time (e.g. Gates et al., 1965; Asner, 1998; Kokaly et al., 2009; Garbulsky et al., 2011). Accurate leaf pigment content can be acquired from visible and near infrared regions of leaf reflectance spectra at wavelengths of 400–700 nm and 700–1400 nm, respectively, generated by hyperspectral imaging (e.g. Gamon and Surfus, 1999; Sims and Gamon, 2002; Gitelson et al., 2009). Leaf pigments are indispensable for photosynthesis as they (i) absorb photosynthetically active radiation, covering the visible portion of the light spectrum, and (ii) partly protect the photosynthetic apparatus against stress such as excess light and low temperatures. Although the basic features of foliar reflectance are widely understood, non-linear and species-specific relations between pigment content and leaf spectral properties hinder upscaling exercises required for large-scale remote sensing applications (Ollinger, 2010). Other leaf properties as nitrogen content, water content and leaf thickness are rather estimated from absorption and scattering in the near infrared region and beyond (>1000 nm; Curran, 1989; Smith et al., 2003; Kokaly et al., 2009).

Through digital imaging optical information can be captured, as "greenness", nitrogen status and therefore photosynthetic capacity of leaves (Woebbecke et al., 1995; Kawashima and Nakatani, 1998; Rorie et al., 2011) and canopies (Blinn et al., 1988; Richardson et al., 2007, 2009a,b). Light intensity quantized in the red, green and blue

* Corresponding author at: University of Antwerp, Biology Department, Research Group Plant and Vegetation Ecology, Universiteitsplein 1, 2610 Wilrijk, Belgium. Tel.: +32 3 265 22 72; fax: +32 3 265 22 71.
E-mail address: Sophie.Dillen@ua.ac.be (S.Y. Dillen).

0168-1923/$ – see front matter © 2012 Elsevier B.V. All rights reserved.
doi:10.1016/j.agrformet.2012.03.001

bands can be extracted from digital images. These values roughly cover the visible spectrum, but overlap for adjacent wavelengths and are not discrete reflectance values for a given wavelength. As a consequence, no specific physiological information, e.g. leaf chlorophyll or xanthophyll content, can be retrieved from digital images as opposed to reflectance spectra.

Several sources explain variability among key biochemical, physiological and anatomical leaf properties, and some of these differences can be tracked by concomitant changes in leaf spectral and optical properties. Cleland et al. (2007) defined phenology as the study of periodic events in life cycles of plants or animals, as influenced by the environment, especially temperature and precipitation changes driven by weather and climate. In foliage of deciduous trees, changes related to phenology and ontogeny, i.e. developmental stage or age, occur in chlorophyll content, leaf mass per unit area, nutrient content, leaf color, photosynthetic capacity, leaf tissue structure, etc. over the course of the growing season (Merzlyak and Gitelson, 1995; Grassi et al., 2005; Poorter et al., 2009). Insight into and precise estimation of these changes are very useful for modeling of carbon assimilation and budget of forests, particularly the seasonal trends of model parameters as V_{cmax}, J_{max}, g_s and R_d (Wilson et al., 2000, 2001; Kosugi et al., 2003; Ito et al., 2006; Mo et al., 2008; Reynolds et al., 2009).

Leaf properties also vary with species (Knapp and Carter, 1998; Wright et al., 2004). Wright et al. (2004) described a universal leaf economics spectrum along which leaf properties alter depending on the leaf growth strategy of plant species, i.e. quick or slow return on investment in nutrients or dry mass in leaves. In this study, two co-occurring temperate deciduous tree species were followed throughout the growing season, i.e. *Quercus rubra* L. (northern red oak) and *Betula papyrifera* Marsh. (paper or white birch). While red oak is a mid- to late-successional tree species in the Northeastern US, paper birch is a typical pioneer species recolonizing disturbed forest areas (Burns and Honkala, 1990). Birch trees are characterized by fast growth rates, high photosynthetic rates and indeterminate growth habit, i.e. continuous leaf production and shoot extension over several weeks or months at the start of the growing season (Bassow and Bazzaz, 1998; Wang and Kimmins, 2002). In contrast, mid- and late-successional trees are often believed to accommodate lower rates of growth and photosynthesis and/or (semi-)determinate growth habit, i.e. a single growth flush at the start of the growing season when a relatively short period of shoot elongation occurs (Marks, 1975; Bassow and Bazzaz, 1997, 1998). We speculate that along the leaf economics spectrum paper birch has a more 'quick-return' strategy in comparison with red oak.

To our knowledge, this is the first study to document leaf reflectance in relation to photosynthetic parameters, V_{cmax} and J_{max}, and other functional properties measured on mature individuals of two co-occurring deciduous tree species over the course over a growing season. In this manuscript the following questions were answered: (i) do phenology and key functional leaf properties differ between two temperate deciduous tree species of different growth habit; (ii) how do leaf spectral, optical, photosynthetic and structural properties relate over the course of the growing season; (iii) do the spectral and optical signatures of leaves reflect their physiology throughout the growing season, and differences therein between the two studied species.

2. Materials and methods

2.1. Experimental site

The study was conducted at Harvard Forest, Petersham (MA; 42°32′N, 72°11′W, elevation 340 m a.s.l.) in a 70- to 80-year-old mixed deciduous stand along the Prospect Hill tract at the EMS annex walk-up tower. At this location, forest composition was dominated by *Q. rubra*, *Acer rubrum* L. (red maple), *Betula lenta* L. (black birch) and *Tsuga canadensis* L. (eastern hemlock). Two abundant, co-occurring species with a contrasting growth habit were chosen for this study, i.e. *Q. rubra* and *B. papyrifera*. Ten representative trees of each of the two species were selected. The trees chosen were typical of the stand size class, about 20 m tall. Three out of the ten individuals were located within 10 m of a small access road. This allowed for tree crown access for leaf-level measurements using an aerial lift. Meteorological data were obtained from the Fisher Meteorological Station located at an open field plot near the experiment (Boose, 2001). Air temperature was recorded at 15-min intervals at 2.2 m above the ground (Vaisala HMP45C, Campbell Scientific Inc., Logan, UT, USA). Precipitation was monitored with a Met One 385 heated rain gage (Campbell Scientific Inc., Logan, UT, USA; top of gage 1.6 m above the ground).

2.2. Ground observations

Phenology observations were made at 4–7 day intervals from April 5 through May 31 and from September 15 through October 30, using the method described by Richardson and O'Keefe (2009). Ground observations were done on all ten individuals per tree species. Three phenological stages were defined: (i) bud break as the date when recognizable leaves appeared from 50% of the buds on an individual; (ii) near-complete leaf development as the date when 50% of the leaves on an individual had reached 75% of their final, mature size and; (iii) leaf fall as the date when 50% of leaves on an individual had dropped (Richardson and O'Keefe, 2009). All dates were derived from linear interpolation between adjacent observations.

2.3. Crown measurements

2.3.1. Phenology observations

From May until October, crown measurements were made on the three accessible mature individuals per species on a monthly basis. From up in the canopy, bud development and shoot growth, i.e. the duration and pattern of shoot growth phases were followed. To this end, a label was attached to five branches of each selected tree during the first field campaign. Leaves emerging between the label and the end of the branch were counted on a monthly basis.

2.3.2. Gas exchange measurements

Each month, three to four leaves were selected in the upper, sunlit crown layer. Leaf gas exchange was measured with a portable open-path gas exchange measurement system (LI-6400, Li-COR, Lincoln, NE, USA). Photosynthetic response to intercellular CO_2 concentration (A_n/C_i) was measured under photosynthetically active radiation (PAR) of 1500 $\mu mol\ m^{-2}\ s^{-1}$ which provides >95% saturation and block temperature was set to 25 °C. Response curves were generated by measuring leaf photosynthesis at ten CO_2 concentrations in the following order: 380 180 100 70 45 380 600 720 1000 and 2000 ppm. Once in a while, dark respiration (R_d) was measured at PAR = 0 $\mu mol\ m^{-2}\ s^{-1}$. During the measurements relative humidity of the leaf chamber was kept between 50 and 80%. Light-saturated photosynthetic rate (A_{sat}) and stomatal conductance (g_s) at CO_2 concentration of 380 ppm and maximum assimilation rate (A_{max}) at 2000 ppm were derived from A_n/C_i curves. Values for the photosynthetic parameters, maximum carboxylation rate (V_{cmax}) and maximum electron transport rate (J_{max}), were estimated from the A_n/C_i curves by fitting the biochemical photosynthesis model of Farquhar et al. (1980) with the least squares method (cf. Appendix

Table 1
Summary of spectral vegetation and color indices used in this study, calculated from leaf spectra and digital images respectively, with their formulae and applications. R_y is the reflectance at a specific wavelength y.

Index	Abreviation	Formula	Application	References
Spectral vegetation indices				
Chlorophyll Normalized Difference Index	Chl NDI	$[R_{750} - R_{705}]/[R_{750} + R_{705}]$	Chlorophyll content	Gitelson et al. (2006, 2009)
Photochemical Reflectance Index	PRI	$[R_{531} - R_{570}]/[R_{531} + R_{570}]$	Carotenoids; xanthophyll cycle	Gamon et al. (1992, 1997)
Red Edge Position	λRE	$\lambda_{max}(dR/d\lambda)$	Chlorophyll content	Curran et al. (1995)
Normalized Difference Vegetation Index	NDVI	$[R_{750} - R_{675}]/[R_{750} + R_{675}]$	Chlorophyll content and energy absorption	Gamon et al. (1997) and Gamon and Surfus (1999)
Color indices				
Green Chromatic Coordinate	g_{cc}	Green/[Red + Green + Blue]	Greenness foliage	Gillespie et al. (1987) and Sonnentag et al. (2012)
Hue	H	See Appendix B	Dominant wavelength in a mixture of light waves	Gonzalez and Woods (1992) and Tang et al. (2000)
Saturation	S	1 − [min(Red, Green, Blue)]/I	Amount of white light mixed with light of given hue	Gonzalez and Woods (1992) and Tang et al. (2000)
Intensity	I	[Red + Green + Blue]/3	Brightness	Gonzalez and Woods (1992) and Tang et al. (2000)

A). Photosynthetic parameters were standardized to 25 °C using Arrhenius equations.

2.3.3. Spectral reflectance and optical measurements

Immediately after gas exchange measurements were made, and on the same leaves, spectral leaf reflectance at wavelengths from 325 to 1075 nm was measured using the FieldSpec HandHeld spectrometer with leaf clip (FS HH, ASD Inc., Boulder, CO, USA). The bare fiber-optic had a field of view of 25°. Before every new leaf sample, dark current and white reference (Spectralon panel) corrections were made. Each leaf scan represented the average of ten passes and the instrument's integration time was set at 68 ms. During the first month's field campaign only, spectral measurements had to be corrected as combined reflectance and transmission of leaves were inadvertently measured. In the visible portion of the light spectrum, we assumed that: $M = R + T^2$ and $R = T$, where M was our measurement with a perfect reflector behind leaf samples, R was the actual reflectance, and T was the transmittance (Jensen, 2007). A quadratic equation established between M and R measured during later field campaigns was used to further correct M values of the first field campaign. Spectral indices derived from leaf spectra are summarized in Table 1.

After spectral reflectance measurements a nadir image was taken from each leaf with a consumer-grade 12.1-megapixel digital camera (Lumix GF1, Panasonic, 4/3-type Live MOS sensor). Pictures of leaves were always taken with the same background, i.e. brown paper bag, with a horizontal orientation of the leaf to camera, but at varying illumination conditions throughout the day and over the growing season. Images were saved in the common compressed JPEG file format. The leaves were extracted by the selection tool of ImageJ, an open source image processing software (Abramoff et al., 2004), and mean red, green and blue (RGB) digital numbers of the selected regions-of-interest were calculated in the *R* statistical computing environment (Language Environment, Version 2.12.1). The RGB color space was converted to HSI, i.e. Hue Saturation Intensity color space (Table 1 and Appendix B). Color indices discussed in this study are summarized in Table 1. Color indices from RGB and HSI color spaces have been successfully applied in assessment of cover, senescence, leaf nitrogen content, etc. (Adamsen et al., 1999; Ewing and Horton, 1999; Jia et al., 2004; Marchand et al., 2004; Sonnentag et al., 2012).

2.3.4. Leaf area, mass and nitrogen

Leaf area (LA) was calculated from digital images of leaves and a known scaling factor using ImageJ. Leaves were dried in a drying oven for 48 h and leaf dry mass was measured in order to define leaf mass per unit area (LMA; leaf dry mass/leaf area). After grinding, leaves were analyzed for nitrogen (N) by a dynamic Flush Combustion Method with a NC 2100 Soil Analyzer (Carlo Erba Strumentazione, Rodano, Italy). From mass-based leaf N content (N_{mass}) and projected leaf area, area-based leaf N content (N_{area}) was calculated.

2.4. Statistical analyses

Data were analyzed in the *R* statistical computing environment. Means and standard errors were calculated on species-level basis. Normality of residuals was tested with the Shapiro–Wilk statistic and if needed, data were adjusted using the Box–Cox method. Effects of seasonality on, and between-species differences in, leaf photosynthetic, reflectance and other biophysical properties were assessed by mixed model repeated measures analysis of variance (ANOVA), with DOY and species as a fixed effects, tree individual as a random effect and species × DOY interaction. The ANOVA was performed twice, i.e. with and without data collected in May. Post hoc evaluation was done by Tukey's HSD test. Two-tailed Student's *t*-tests were used to test differences in phenology between species. Relationships between spectral vegetation index λRE and leaf functional traits were evaluated by calculation of Pearson correlation coefficients (r) on leaf-level basis. To test whether V_{cmax}–λRE and V_{cmax}–N_{area} relationships differed among species, we performed an analysis of covariance (ANCOVA) with V_{cmax} as dependent variable, λRE and N_{area} as covariates and species as categorical variable.

3. Results

3.1. Weather and soil water content

Phenological studies require basic information on environmental conditions driving leaf functional traits throughout the growing season. Seasonal variation in daily average air temperature and in precipitation is presented in function of day of year (DOY) in Fig. 1. The year 2010 was characterized by a exceptionally warm spring and summer (Boose, 2001). In general, soil water is always available to deep-rooting mature trees at Harvard Forest.

3.2. Species-specific differences

The average date of bud break was seven days earlier in paper birch than in red oak (Table 2). Overall, bud break at Harvard Forest was about 10–14 days earlier in 2010 than the average bud break over a 20-year period (John O'Keefe, pers. communication). Accordingly, paper birch rapidly expanded its leaves and reached mature leaf size 13 days earlier than red oak (Table 2). Shoot apices of paper

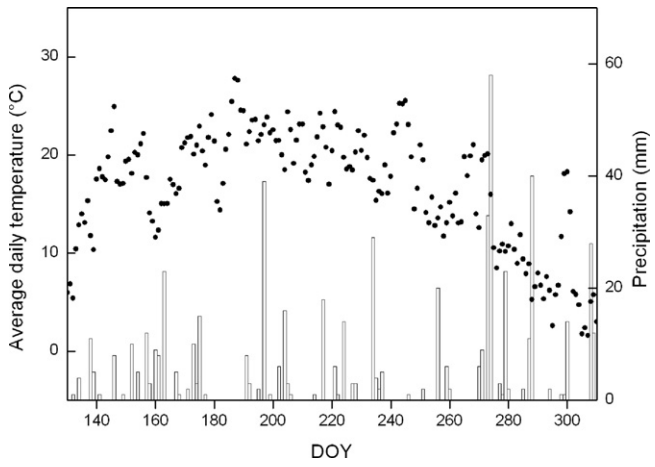

Fig. 1. Average daily temperature and precipitation in function of day of year (DOY) measured at the meteorological station located at Harvard Forest during the growing season of 2010.

Table 2
Phenological events expressed in day of years (DOY, mean ± standard error), except for length of growing season.

Phenological event	*Betula papyrifera*	*Quercus rubra*	*t*	*df*	*P*
Bud break (DOY)	107 ± 1	114 ± 1	−5.97	26	**
Near-complete leaf expansion (DOY)	122 ± 1	135 ± 1	−26.1	17	**
50% leaf fall (DOY)	290 ± 1	297 ± 1	−3.63	24	*
Growing season length (days)	183 ± 1	182 ± 1	−0.144	24	ns

Results of Student's *t*-tests (degrees of freedom (*df*), *t*- and *P*-values) are indicated. ns = not significant.
* $P \leq 0.01$
** $P \leq 0.001$.

birch continued producing leaves and growing until late June, while red oak had typically one short flush of leaves at the start of the growing season (results not shown). Yet, in both species, shoot elongation ceased in early summer (June–July). Autumn senescence and leaf fall were first visible in paper birch, about five days earlier than in red oak. The length of the growing season did not differ significantly between the two tree species (Table 2).

The repeated measures ANOVA indicated significant species differences maintained over the summertime and fall for the majority of the studied leaf properties (Table 3; Figs. 2 and 3). From late June to late October, red oak exhibited significantly larger leaves, higher A_{sat}, g_s, V_{cmax}, N_{mass} and N_{area}, and higher values for spectral vegetation indices Chl NDI, λRE and PRI or Photochemical Reflectance Index (see Table 1). Since J_{max} was similar in birch and oak, the ratio J_{max}:V_{cmax} was significantly larger in paper birch (Table 3). Significant species × DOY interactions were observed for many traits (Table 3). However, stronger species × DOY interactions were obtained when data collected late May were included in the analysis (results not shown). The different timing of bud break and onset of senescence of two species explained most of this strongly species-specific behavior over time. At the end of May, oak leaves were still expanding and displayed markedly different spectral, physiological and biochemical properties as compared to fully expanded birch leaves (Figs. 2 and 3). From the crown measurements in May, oak leaves had higher reflectance in the visible portion of the light spectrum, lower photosynthetic rates and capacity, lower N_{area} and lower chlorophyll content as indicated by reflectance indices, Chl NDI and λRE as compared to birch leaves (Figs. 2 and 3).

3.3. Seasonal variation

The rapid rise in LMA from May to June indicated that red oak leaves thickened during this period (Fig. 2). LMA continued increasing at a slower rate until the end of August for the red oak leaves, while birch leaves displayed relatively stable values of LMA (Fig. 2). N_{area} followed a strikingly different seasonal pattern as compared to N_{mass} because of the steady increase of LMA at the start of the growing season ($N_{area} = N_{mass} \cdot LMA$). Photosynthetic values and stomatal conductance followed a bell-shaped seasonal pattern in both species, typical of deciduous trees (Fig. 2). Generally, maximum values were reached after completion of leaf expansion end of June till onset of senescence mid- to late September (Fig. 2) and, subsequently, were maintained for two to three months. The

Table 3
Least square means ± standard error for all photosynthetic, structural and biochemical leaf properties of *Betula papyrifera* and *Quercus rubra*, and indices calculated from leaf spectra from late June till late October.

	Trait	Between-species differences					Species × DOY	
		Betula papyrifera Mean ± SE		*Quercus rubra* Mean ± SE	*F*	*P*	*F*	*P*
Gas exchange	A_{sat}	9.07 ± 0.47	<	11.55 ± 0.47	14.89	***	3.46	*
	A_{max}	23.62 ± 0.92		25.81 ± 0.94	2.91	0.09	6.57	***
	g_s	0.16 ± 0.01	<	0.23 ± 0.01	15.77	***	3.35	*
	V_{cmax}	55.35 ± 1.98	<	73.15 ± 2.11	30.44	***	1.62	ns
	J_{max}	107.87 ± 3.11		107.62 ± 3.23	0.00	ns	2.79	*
	J_{max}:V_{cmax}	2.07 ± 0.04	>	1.75 ± 0.05	47.6	***	0.30	ns
Leaf morphology	LA	28.0 ± 3.6	<	115.6 ± 3.5	281.3	***	0.81	ns
	LMA	78.25 ± 2.10	<	97.46 ± 2.35	27.78	***	2.15	ns
Leaf nitrogen	N_{mass}	17.58 ± 0.33	<	20.25 ± 0.38	13.39	***	3.51	*
	N_{area}	1.33 ± 0.05	<	1.99 ± 0.06	48.11	***	2.52	ns
Spectral vegetation indices	λRE	703.44 ± 0.65	<	707.00 ± 0.67	13.99	***	1.03	ns
	Chl NDI	0.40 ± 0.01	<	0.43 ± 0.01	6.42	*	3.01	*
	PRI	−0.020 ± 0.004	<	−0.007 ± 0.004	4.39	*	4.15	**
	NDVI	0.82 ± 0.00		0.83 ± 0.00	0.30	ns	0.25	ns

F- and *P*-values from repeated measures ANOVA are given. ns = not significant. Definitions: A_{sat} is light-saturated assimilation rate ($\mu mol\, m^{-2}\, s^{-1}$); A_{max} is maximum assimilation rate ($\mu mol\, m^{-2}\, s^{-1}$); g_s is stomatal conductance ($mol\, m^{-2}\, s^{-1}$); V_{cmax} is maximum carboxylation rate ($\mu mol\, m^{-2}\, s^{-1}$); J_{max} is maximum electron transport rate ($\mu mol\, m^{-2}\, s^{-1}$); LA is individual leaf area (cm^2); LMA is leaf dry mass per unit leaf area ($g\, m^{-2}$); N_{mass} is mass-based leaf nitrogen ($mg\, g^{-1}$); N_{area} is area-based leaf nitrogen ($g\, m^{-2}$); λRE is Red Edge Position (nm); Chl NDI is Chlorophyll Normalized Difference Index; PRI is Photochemical Reflectance Index; NDVI is Normalized Difference Vegetation Index.
* $P \leq 0.05$
** $P \leq 0.01$.
*** $P \leq 0.001$.

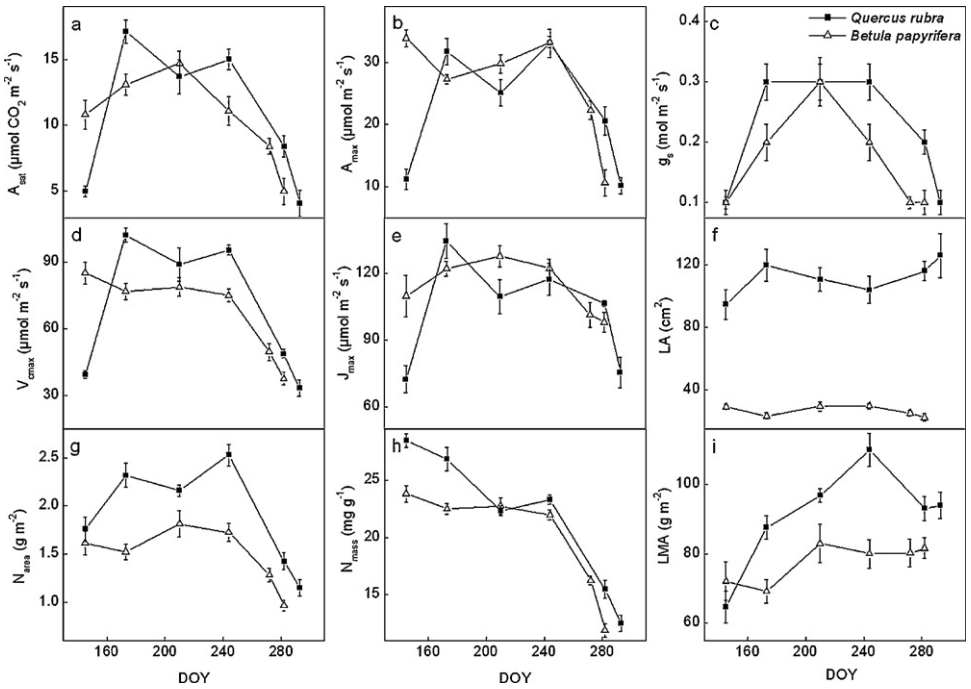

Fig. 2. Leaf gas exchange and other leaf properties in function of day of year (DOY) for *Quercus rubra* (■) and *Betula papyrifera* (△). Means and standard errors are given (n = 3–5). Definitions: (a) A_{sat} is light-saturated assimilation rate; (b) A_{max} is maximum assimilation rate; (c) g_s is stomatal conductance; (d) V_{cmax} is maximum carboxylation rate; (e) J_{max} is maximum electron transport rate; (f) LA is individual leaf area; (g) N_{area} is area-based leaf nitrogen; (h) N_{mass} is mass-based leaf nitrogen; (e) LMA is leaf dry mass per unit area.

ratio J_{max}:V_{cmax} followed a very distinct pattern: values of 1.2–1.5 were relatively stable through spring and summer, but a strong increase to values of 2.4–2.8 was observed from late September onward.

Seasonal trends of Chl NDI and λRE indicate that the chlorophyll pool was at its largest toward July and August (Fig. 3). First signs of leaf aging and senescence were apparent in paper birch leaves. Late September, birch leaves already showed strong drops

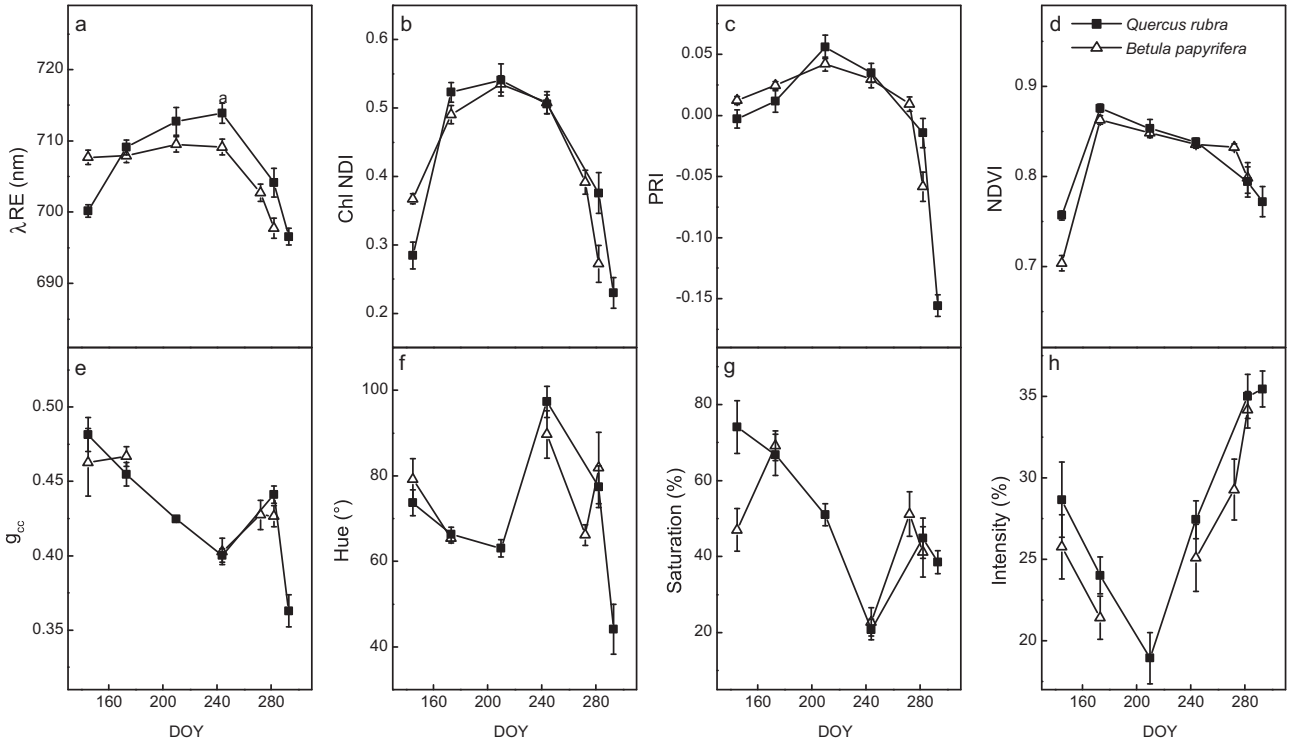

Fig. 3. Spectral vegetation indices (upper panels) and color indices (lower panels) in function of day of year (DOY) for *Quercus rubra* (■) and *Betula papyrifera* (△). Means and standard errors are given (n = 3–5). Definitions: (a) λRE is Red Edge Position; (b) Chl NDI is Chlorophyll Normalized Difference Index; (c) PRI is Photochemical Reflectance Index; (d) NDVI is Normalized Difference Vegetation Index; (e) g_{cc} is Green Chromatic Coordinate; (f) Hue; (g) Saturation; (h) Intensity.

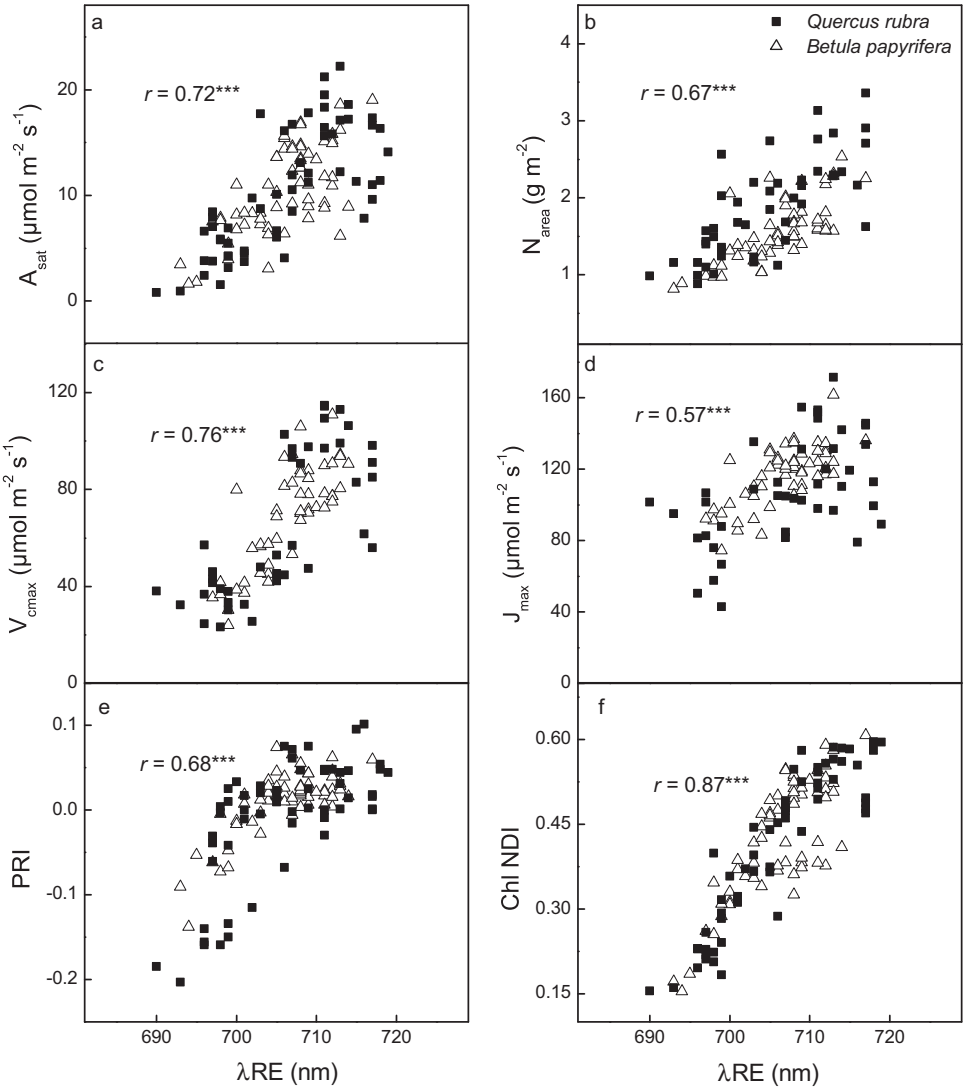

Fig. 4. Relationships between spectral vegetation index λRE (Red Edge position) and key functional leaf traits as well as other spectral indices. (a) A_{sat} is light-saturated assimilation rate; (b) N_{area} is area-based leaf nitrogen; (c) V_{cmax} is maximum carboxylation rate; (d) J_{max} is maximum electron transport rate; (d) PRI is Photochemical Reflectance Index; (e) Chl NDI is Chlorophyll Normalized Difference Index. Pearson correlation coefficients (r) and significance levels are presented. ***$P \leq 0.001$.

in Chl NDI and λRE indicating chlorophyll breakdown. NDVI and PRI behaved somewhat differently throughout the growing season; both reflectance vegetation indices exhibited more asymmetrical seasonal patterns as compared to Chl NDI and λRE. Green leaf color was evident from both the Green Chromatic Coordinate (g_{cc}) and Hue (H) throughout the growing season, except for oak leaves in the fall which were characterized by low g_{cc} and low H values indicating their reddish color (Fig. 3). Saturation (S) or the brightness of the green color decreased throughout the growing season. Intensity (I) was lowest in summer (Fig. 3).

3.4. Correlations

Various relationships were found among measured traits. Correlation coefficients between photosynthesis and nitrogen on a mass basis were slightly lower than coefficients calculated on an area basis (results not shown). From the studied spectral vegetation indices, λRE, showed strongest correlations and was linearly related with key functional leaf traits (Fig. 4). Chl NDI and PRI were positively but not linearly related to photosynthesis traits, indirectly shown by their non-linear relationship with λRE (Fig. 4). Moderate correlation coefficients were found between spectral indicators of chlorophyll and N_{area}, confirming mobilization of nitrogen is coupled to the production and breakdown of chlorophyll. LMA did not correlate with photosynthesis, λRE or other indices. The V_{cmax}–λRE relationship did not significantly differ between the two species as opposed to V_{cmax}–N_{area} (Table 4). N_{area} explained about 48 and 55% of the variation in V_{cmax}, for birch

Table 4
Results of the F-test performed on the ANCOVA for maximum carboxylation rate (V_{cmax}) with Red Edge Position (λRE; panel a) and area-based nitrogen content (N_{area}; panel b) as covariates and species as categorical variable.

	df	*F*-value	
(a)			
λRE	1	118.0	***
Species	1	0.1	ns
λRE × species	1	1.1	ns
Residuals	86		
(b)			
N_{area}	1	78.0	***
Species	1	15.0	***
N_{area} × species	1	0.1	ns
Residuals	80		

*** $P \leq 0.001$

and oak respectively. λRE explained up to 57% of the variation in V_{cmax} for both species over the course of the growing season. No significant correlations were obtained between color indices and other studied leaf traits, except for color index Intensity (I) which was negatively associated with photosynthesis, area-based nitrogen content and spectral vegetation indices (r ranging from −0.27 to −0.46 and $P \leq 0.001$).

4. Discussion

4.1. Species differences in leaf properties

Phenological timing and between-species differences therein are crucial for the competitive ability and survival of a given tree species (Murray and Ceulemans, 1998). The ranking of phenological timing among species is known to remain fairly consistent over a 20-year period of phenological observations at Harvard Forest, in particular for spring phenology (John O'Keefe, pers. communication). The relatively early bud break and rapid leaf expansion in paper birch may be a function of its intolerance to shade, growth habit and/or wood anatomy (Lechowicz, 1984; Polgar and Primack, 2011). Paper birch has diffuse-porous wood and indeterminate growth. Both features diminish damage risks of late frosts as loss of hydraulic conductivity caused by cavitation and loss of foliage, and can be associated with early bud break as opposed to trees with ring-porous wood and determinate growth (Lechowicz, 1984; Sanz-Pérez et al., 2009).

Our results revealed different functional leaf properties between mature individuals of the two studied species over the course of the growing season, partly due to species-specific phenology. Fully expanded oak leaves combined higher A_{sat} and V_{cmax} with higher leaf nitrogen content and LMA as compared to paper birch. Yet, along the leaf economics spectrum, paper birch appeared to be quite similar to red oak. According to the leaf economics spectrum, plant species with dense leaves or high LMA often have longer leaf life spans and lower N_{mass} and A_{mass}, i.e. high invest, slow return strategy (Wright et al., 2004). On the other side of the spectrum, plants species with thin leaves or low LMA have shorter leaf life spans, higher N_{mass} and A_{mass}, i.e. low invest, rapid return strategy. During the summertime (July–August), oak leaves had significantly higher LMA and N_{mass}. A_{mass} was not significantly different between mature individuals of the two species during this period of the year (data not shown). Simultaneous measurements on two-year-old paper birch and red oak saplings in a nearby clear-cut stand yielded contrasting results (unpublished results). Birch saplings displayed higher A_{mass}, N_{mass} and lower LMA values or, in other words, were more at the rapid return side of the leaf economics spectrum than oak saplings. In summary, these findings suggest that tree age may affect tree and leaf growth strategy and leaf functional traits as well as their mutual relations.

4.2. Seasonal variation

The observed seasonal variation in photosynthetic capacity and other leaf functional properties was consistent with previous studies on deciduous trees (Bassow and Bazzaz, 1998; Wilson et al., 2001; Kosugi et al., 2003; Ito et al., 2006; Grassi et al., 2005; Reynolds et al., 2009). Seasonal changes of red oak and paper birch were comparable, except in May due to species-specific phenology and in July due to a drop in photosynthesis in oak. Since we only measured at a monthly basis during short intensive field campaigns, the seasonal pattern was composed of a limited number of observations. Therefore, we could not demonstrate the persistence of the drop in photosynthetic parameters of oak leaves in July. Lowest photosynthetic rates and capacity were recorded during leaf expansion in spring and senescence in fall, under unrestricted water availability at Harvard Forest. The peak values of A_{sat}, V_{cmax} and J_{max} were maintained till middle to late August as found for A_{sat} in 1992 by Bassow and Bazzaz (1998).

Bud break in the studied species was about three weeks earlier in 2010 than in 1992 (cf. Bassow and Bazzaz, 1998). The warm, early spring of 2010 advanced the start of the growing season with about three weeks as compared to 1992. This strong year-to-year difference in phenology was reflected by spring photosynthesis values of red oak leaves; in 2010 peak A_{sat} values were recorded late June. In 1992, A_{sat} only reached peak values in mid-July. No differences in spring photosynthesis were observed for paper birch, since it is characterized by early bud break and no data were available for May 1992. Despite substantial differences in leaf age, date of leaf drop and fall photosynthesis values were not markedly different between the two studies. A warm and early spring likely results in a longer growing season and increased canopy productivity of most dominant deciduous tree species at Harvard Forest. Indeed, in this region year-to-year variation in canopy photosynthesis has been mainly contributed to variation in climatic conditions, more specifically ambient temperature especially in spring time (Goulden et al., 1996; Richardson et al., 2009a).

4.3. Spectral reflectance and optical indicators of leaf physiology

Photosynthetic rates and capacity were rather a result of leaf nitrogen than leaf thickness over the course of the growing season. In deciduous trees, where greenness of the canopy closely coincides with both leaf nitrogen and photosynthetic capacity, greenness or chlorophyll indices as NDVI, Chl NDI, λRE or CI (Chlorophyll Index) are most effective. From the studied indices, Chl NDI and λRE, gave a good indication of photosynthetic capacity. However, λRE performed best at tracking seasonal and species differences. At high levels of chlorophyll, some spectral vegetation indices may perform poorly and not differentiate well given non-linear relationships with leaf chlorophyll content (Richardson et al., 2002). This could explain why Chl NDI and NDVI did not differentiate between species in July and August at peak values of leaf gas exchange and nitrogen. In evergreen species, PRI is a promising indicator of xanthophyll cycle pigment activity and, thus, radiation use efficiency, but these relations can be masked by seasonal changes in carotenoid to chlorophyll ratios in deciduous trees and are often influenced by the time scale of the measurements (Hilker et al., 2011). Indeed, over the course of the growing season PRI generally gave a poorer indication of photosynthesis in comparison with λRE (results not shown) illustrating that PRI cannot be replaced by λRE or other indices. Nonetheless, the relationship between PRI and J_{max} warrants further study since the downregulation of the J_{max} is coupled to an increase in non-photochemical quenching of chlorophyll fluorescence (NPQ; Weis and Berry, 1987) where xanthophyll cycle pigments have an important role (Niyogi, 1999).

Changes in leaf or canopy color over time can be tracked at a low cost with digital imaging (Woebbecke et al., 1995; Kawashima and Nakatani, 1998; Ahrends et al., 2008; Richardson et al., 2007, 2009b; Sonnentag et al., 2012). The highly variable light conditions and the limited number of digital images hampered to some extent the interpretation of the color indices derived from the RGB and HSI color spaces. All color indices, i.e. g_{cc}, H, S and I, displayed distinct seasonal patterns from leaf photosynthesis and spectral vegetation indices. Consequently, few relationships were obtained between color indices and other studied traits. In the middle of the growing season, highest photosynthetic activity and absorption was recorded on dark green leaves with low I. Yet, color index I should be interpreted with care since it is very sensitive to illumination conditions. The potential of g_{cc} as measure of leaf greenness and functioning appeared to be limited in

this study, mainly because expanding leaves combine high g_{cc} (or greenness) with low photosynthetic rates. However, g_{cc} at canopy level simultaneously assessed by Sonnentag et al. (2012) showed more potential. Obviously, our leaf images were not fully exchangeable with high-frequency repeat photography to continuously track phenology or physiology of canopies or tree crowns due to the impact of canopy structure, total leaf area index and leaf angle on canopy or tree crown observations (Richardson et al., 2007, 2009b).

In conclusion, seasonal variability in foliar reflectance and leaf physiology was comparable between the two species, except early in the growing season since bud break of paper birch occurred significantly earlier compared to red oak. As most pronounced differences in leaf photosynthetic capacity and foliar reflectance occurred during bud break and leaf development, large species variation in phenology could favor species identification through remote sensing at key points in the growing season as highlighted by Castro and Sanchez-Azofeifa (2008). Spectral vegetation indices λRE and Chl NDI showed potential as indicators of key functional leaf properties as N_{area}, A_{sat} and V_{cmax} throughout the growing season. A common relationship between foliar reflectance and photosynthetic capacity was demonstrated for both species. Optical information obtained through digital imaging should be interpreted with care since color indices do not follow the typical bell-shaped seasonal patterns as observed for many leaf properties as photosynthetic capacity, area-based nitrogen content and spectral vegetation indices.

Acknowledgments

The authors acknowledge Eli Melaas, Heidi Renninger, Leah Nagel, John O'Keefe, Thomas Gibaud, Lucas Griffith and Harvard Forest staff for field assistance, Prof. Alan Strahler for the use of the spectrometer and Prof. Adrien Finzi and his lab for the nitrogen analyses. S.Y. Dillen is a post-doctoral research associate of the Fund for Scientific Research-Flanders (F.W.O.-Vlaanderen, Belgium).

Appendix A. Biochemical photosynthesis model.

Maximum carboxylation rate per unit leaf area (V_{cmax}) and maximum electron transport rate (J_{max}) were estimated from A_n/C_i curves applying the biochemical photosynthesis model of Farquhar et al. (1980). According to this model net assimilation rate is limited by Rubisco (or nitrogen, A_c) at low C_i exposure and hence assimilation can be calculated as:

$$A_c = \frac{V_{cmax}(C_i - \Gamma')}{C_i + K_c(1 + 0/K_o)} - R_d$$

where Γ' is the CO_2 compensation point in absence of mitochondrial respiration, O is the intercellular O_2 concentration, K_c and K_o are the Michaelis–Menten constants of Rubisco for CO_2 and O_2, respectively, R_d is leaf dark respiration.

At higher levels of C_i, net assimilation rate is limited by RuBP regeneration and A_j is defined as:

$$A_j = \frac{J(C_i - \Gamma')}{4C_i + 8\Gamma'} - R_d$$

At light saturation, J is equal to J_{max}, but at lower light levels J may be estimated from (von Caemmerer, 2000):

$$J = \frac{\alpha + J_{max} - \sqrt{(\alpha + J_{max})^2 - 4\Theta\alpha J_{max}}}{2\Theta}$$

where Θ is the curvature of leaf response of electron transport to PAR and α is the absorption of PAR by leaves.

Parameters R_d, Γ', K_c and K_o are temperature-dependent and calculated from reference values at 25 °C, applying an Arrhenius equation:

$$x = x_{25} \exp\left(\frac{E_a(T - 25)}{298R(T + 273)}\right)$$

where x is the parameter value, x_{25} is the parameter value at 25 °C. For V_{cmax} and J_{max}, this equation is extended to:

$$x = x_{25} \exp\left(\frac{\Delta H_a(T - 25)}{298R(T + 273)}\right) \frac{\left(1 + \exp\left[(298\Delta S - \Delta H_d)/298R\right]\right)}{\left(1 + \exp\left[((T + 273)\Delta S - \Delta H_d)/(T + 273)R\right]\right)}$$

where ΔS is the entropy term, ΔH_a is the activation energy, T is the temperature, R is the universal gas constant and ΔH_d is the deactivation energy. Reference values at 25 °C with their activation energies and input parameter values are listed in Supplementary Table S1 (Bernacchi et al., 2001; De Pury and Farquhar, 1997; Evans, 1987; Harley et al., 1992; Jones, 1992).

Appendix B. Conversion of RGB to HSI color system.

If $G \geq B$,

$$\text{Hue} = \arccos\left\{\frac{[(R - G) + (R - B)]/2}{\sqrt{\left((R - G)^2\right)/[(R - G)(G - B)]}}\right\}$$

If $G < B$,

$$\text{Hue} = 360 - \arccos\left\{\frac{[(R - G) + (R - B)]/2}{\sqrt{\left((R - G)^2\right)/[(R - G)(G - B)]}}\right\}$$

Appendix C. Supplementary data

Supplementary data associated with this article can be found, in the online version, at doi:10.1016/j.agrformet.2012.03.001.

References

Abramoff, M.D., Magalhaes, P.J., Ram, S.J., 2004. Image processing with ImageJ. Biophotonics Int. 11, 36–42.
Adamsen, F.J., Pinter, P.J., Barnes, E.M., LaMorte, R.L., Wall, G.W., Leavitt, S.W., Kimball, B.A., 1999. Measuring wheat senescence with a digital camera. Crop Sci. 39, 719–724.
Ahrends, H.E., Brügger, R., Stöckli, R., Schenk, J., Michna, P., Jeanneret, F., Wanner, H., Eugster, W., 2008. Quantitative phenological observations of a mixed beech forest in northern Switzerland with digital photography. J. Geophys. Res. Biogeosci. 11, 3, doi:10.1029/2007JG000650.
Asner, G.P., 1998. Biophysical and biochemical sources of variability in canopy reflectance. Remote Sens. Environ. 64, 234–253.
Bassow, S.L., Bazzaz, F.A., 1997. Intra- and interspecific variation in canopy photosynthesis in a mixed deciduous forest. Oecologia 109, 507–515.
Bassow, S.L., Bazzaz, F.A., 1998. How environmental conditions affect canopy leaf-level photosynthesis in four deciduous tree species. Ecology 79, 2660–2675.
Bernacchi, C.J., Singsaas, E.L., Pimentel, C., Portis Jr., A.R., Long, S.P., 2001. Improved temperature response functions for models of Rubisco-limited photosynthesis. Plant Cell Environ. 24, 253–259.
Blinn, C.R., Lyons, A., Buckner, E.R., 1988. Color aerial photography for assessing need for fertilizers in loblolly pine plantations. South. J. Appl. Forest. 12, 270–273.
Boose, E., 2001. Fisher Meteorological Station (Since 2001). Harvard Forest Data Archive.
Burns, R.M., Honkala, B.H., 1990. Silvics of North American Trees, vol. 2. Hardwoods. US Department of Agriculture, Washington, DC.
Castro, K.L., Sanchez-Azofeifa, G.A., 2008. Changes in spectral properties, chlorophyll content and internal mesophyll structure of senescing *Populus balsamifera* and *Populus tremuloides* leaves. Sensors 8, 51–69.
Cleland, E.E., Chuine, I., Menzel, A., Mooney, H.A., Schwartz, M.D., 2007. Shifting plant phenology in response to global change. Trends Ecol. Evol. 22, 357–365.
Curran, P.J., 1989. Remote sensing of foliar chemistry. Remote Sens. Environ. 30, 271–278.
Curran, P.J., Windham, W.R., Gholz, H.L., 1995. Exploring the relationship between reflectance red edge and chlorophyll concentration in slash pine leaves. Tree Physiol. 15, 203–206.

De Pury, D.G.G., Farquhar, G.D., 1997. Simple scaling of photosynthesis from leaves to canopies without the errors of big-leaf models. Plant Cell Environ. 20, 537–557.
Evans, J.R., 1987. The relationship between electron transport components and photosynthetic capacity in pea leaves grown at different irradiances. Aust. J. Plant Physiol. 15, 59–68.
Ewing, R.P., Horton, R., 1999. Quantitative color image analysis of agronomic images. Agron. J. 91, 659–660.
Farquhar, G.D., von Caemerrer, S., Berry, J.A., 1980. A biochemical model of photosynthetic CO_2 assimilation in leaves of C_3 species. Planta 149, 78–90.
Gamon, J.A., Surfus, J.S., 1999. Assessing leaf pigment content and activity with a reflectometer. New Phytol. 143, 105–117.
Gamon, J.A., Peñuelas, J., Field, C.B., 1992. A narrow-waveband spectral index that tracks diurnal changes in photosynthetic efficiency. Remote Sens. Environ. 41, 35–44.
Gamon, J.A., Serrano, L., Surfus, J.S., 1997. The photochemical reflectance index: an optical indicator of photosynthetic radiation use efficiency across species, functional types, and nutrient levels. Oecologia 112, 492–501.
Garbulsky, M.F., Peñuelas, J., Gamon, J., Inoue, Y., Filella, I., 2011. The photochemical reflectance index (PRI) and the remote sensing of leaf, canopy and ecosystem radiation use efficiencies. A review and meta-analysis. Remote Sens. Environ. 115, 281–297.
Gates, D.M., Keegan, H.J., Schleter, J.C., Weidner, V.R., 1965. Spectral properties of plants. Appl. Opt. 4, 11–20.
Gillespie, A.R., Kahle, A.B., Walker, R.E., 1987. Color enhancement of highly correlated images. 2. Channel ratio and chromaticity transformation techniques. Remote Sens. Environ. 22, 343–365.
Gitelson, A.A., Keydan, G.P., Merzlyak, M.N., 2006. Three-band model for noninvasive estimation of chlorophyll, carotenoids, and anthocyanin contents in higher plant leaves. Geophys. Res. Lett. 33, L11402.
Gitelson, A.A., Chivkunova, O.B., Merzlyak, M.N., 2009. Nondestructive estimation of anthocyanins and chlorophylls in anthocyanic leaves. Am. J. Bot. 96, 1861–1868.
Gonzalez, R.C., Woods, R.E., 1992. Digital Image Processing. Addison-Wesley Publishing, Boston, p. 716.
Goulden, M.L., Munger, J.W., Fan, S.-M., Daube, B.C., Wofsy, S.C., 1996. Exchange of carbon dioxide by a deciduous forest: response to interannual climate variability. Science 271, 1576–1578.
Grassi, G., Vicinelli, E., Ponti, F., Cantoni, L., Magani, F., 2005. Seasonal and interannual variability of photosynthetic capacity in relation to leaf nitrogen in a deciduous forest plantation in northern Italy. Tree Physiol. 25, 349–360.
Harley, P.C., Loreto, F., Di Marco, G., Sharkey, T.D., 1992. Theoretical considerations when estimating mesophyll conductance to CO_2 flux by analysis of the response of photosynthesis to CO_2. Plant Physiol. 98, 1429–1436.
Hilker, T., Gitelson, A., Coops, N.C., Hall, F.G., Black, T.A., 2011. Tracking plant physiological properties from multi-angular tower-based remote sensing. Oecologia 165, 865–876.
Ito, A., Muraoka, H., Koizumi, H., Saigusa, N., Murayama, S., Yamamoto, S., 2006. Seasonal variation in leaf properties and ecosystem carbon budget in a cool-temperate deciduous broad-leaved forest: simulation analysis at Takayama site, Japan. Ecol. Res. 21, 137–149.
Jensen, J.R., 2007. Remote Sensing of the Environment: An Earth Resource Perspective, second ed. Prentice-Hall, Upper Saddle River.
Jia, L., Buerkert, A., Chen, X., Roemheld, V., Zhang, F., 2004. Low-altitude aerial photography for optimum N fertilization of winter wheat on the North China Plain. Field Crop Res. 89, 389–395.
Jones, H.G., 1992. Plants and Microclimate, second ed. Cambridge University Press, Cambridge.
Kawashima, S., Nakatani, M., 1998. An algorithm for estimating chlorophyll content in leaves using a video camera. Ann. Bot. 81, 49–54.
Knapp, A.K., Carter, G.A., 1998. Variability in leaf optical properties among 26 species from a broad range of habitats. Am. J. Bot. 85, 940–946.
Kosugi, Y., Shibata, S., Kobashi, S., 2003. Parametrization of the CO_2 and H_2O gas exchange of several temperate deciduous broad-leaved trees at the leaf scale considering seasonal changes. Plant Cell Environ. 26, 285–301.
Kokaly, R.F., Asner, G.P., Ollinger, S.V., Martin, M.E., Wessman, C.A., 2009. Characterizing canopy biochemistry from imaging spectroscopy and its application to ecosystem studies. Remote Sens. Environ. 113, 78–91.
Lechowicz, M.J., 1984. Why do temperate deciduous trees leaf out at different times? Adaptation and ecology of forest communities. Am. Nat. 124, 821–842.
Marchand, F.L., Nijs, I., Heuer, M., Mertens, S., Kockelbergh, F., Pontailler, J.Y., Impens, I., Beyens, L., 2004. Climate warming postpones senescence in high arctic tundra. Arct. Antarct. Alp. Res. 36, 390–394.
Marks, P.L., 1975. On the relation between extension growth and successional status of deciduous trees of the northeastern United States. Bull. Torrey Bot. Club 102, 172–177.
Merzlyak, M.N., Gitelson, A.A., 1995. Why and what for the leaves are yellow in autumn? On the interpretation of optical spectra of senescing leaves (*Acer platanoides* L.). J. Plant Physiol. 145, 315–320.
Mo, X., Chen, J.M., Ju, W., Black, T.A., 2008. Optimization of ecosystem model parameters through assimilating eddy covariance flux data with an ensemble Kalman Filter. Ecol. Model. 217, 157–173.
Murray, M.B., Ceulemans, R., 1998. Will tree foliage be larger and live longer? In: Jarvis, P.G. (Ed.), European Forests and Global Change. The Likely Impacts of Rising CO_2 and Temperature. Cambridge University Press, Cambridge, pp. 94–125.
Niyogi, K.K., 1999. Photoprotection revisited: genetic and molecular approaches. Ann. Rev. Plant Physiol. Plant Mol. Biol. 50, 333–359.
Ollinger, S.V., 2010. Sources of variability in canopy reflectance and the convergent properties of plants. New Phytol. 189, 375–394.
Pallardy, S.G., Kozlowski, T.T., 2008. Physiology of Woody Plants. Academic Press, San Diego.
Polgar, C.A., Primack, R.B., 2011. Leaf-out phenology of temperate woody plants: from trees to ecosystems. New Phytol. 191, 926–941.
Poorter, H., Niinemets, Ü., Poorter, L., Wright, I.J., Villar, R., 2009. Causes and consequences of variation in leaf mass per area (LMA): a meta-analysis. New Phytol. 182, 565–588.
Reynolds, R.F., Bauerle, W.L., Wang, Y., 2009. Simulating carbon dioxide exchange rates of deciduous tree species: evidence for a general pattern in biochemical ranges and water stress response. Ann. Bot. 104, 775–784.
Richardson, A.D., O'Keefe, J., 2009. Phenological differences between understory and overstory: a case study using the long-term Harvard Forest records. In: Noormets, A. (Ed.), Phenology of Ecosystem Processes: Applications in Global Change Research. Springer, New York, pp. 87–117.
Richardson, A.D., Duigan, S.P., Berlyn, G.P., 2002. An evaluation of noninvasive methods to estimate foliar chlorophyll content. New Phytol. 153, 185–194.
Richardson, A.D., Jenkins, J.P., Braswell, B.H., Hollinger, D.Y., Ollinger, S.V., Smith, M.-L., 2007. Use of digital webcam images to track spring green-up in a deciduous broadleaf forest. Oecologia 152, 323–334.
Richardson, A.D., Hollinger, D.Y., Dail, D.B., Lee, J.T., Munger, J.W., O'Keefe, J., 2009a. Influence of spring phenology on seasonal and annual carbon balance in two contrasting New England forests. Tree Physiol. 29, 321–331.
Richardson, A.D., Braswell, B.H., Hollinger, D.Y., Jenkins, J.P., Ollinger, S.V., 2009b. Near-surface remote sensing of spatial and temporal variation in canopy phenology. Ecol. Appl. 19, 1417–1428.
Rorie, R.L., Purcell, L.C., Mozaffari, M., Karcher, D.E., King, C.A., Marsh, M.C., Longer, D.E., 2011. Association of greenness in corn with yield and leaf nitrogen concentration. Agron. J. 103, 529–535.
Sanz-Pérez, V., Castro-Diez, P., Valladares, F., 2009. Differential and interactive effects of temperature and photoperiod on budburst and carbon reserves in two co-occurring Mediterranean oaks. Plant Biol. 11, 142–151.
Sims, D.A., Gamon, J.A., 2002. Relationships between leaf pigment content and spectral reflectance across a wide range of species, leaf structures and developmental stages. Remote Sens. Environ. 81, 337–354.
Smith, M.-L., Martin, M.E., Plourde, L., Ollinger, S.V., 2003. Analysis of hyperspectral data for estimation of temperate forest canopy nitrogen concentration: comparison between an airborne (AVIRIS) and a spaceborne (Hyperion) sensor. IEEE Trans. Geosci. Remote Sens. 41, 1332–1337.
Sonnentag, O., Hufkens, K., Teshera-Sterne, C., Young, A.M., Friedl, M., Braswell, B.H., Milliman, T., O'Keefe, J., Richardson, A.D., 2012. Digital repeat photography for phenological research in forest ecosystems. Agric. For. Meteor. 152, 159–177.
Tang, L., Tian, L., Steward, B.L., 2000. Color image segmentation with genetic algorithm for in field weed sensing. Trans. ASAE 43, 1019–1027.
von Caemmerer, S., 2000. Biochemical Models of Leaf Photosynthesis. CSIRO Publishing, Collingwood.
Wang, J.R., Kimmins, J.P., 2002. Height growth and competitive relationship between paper birch and Douglas-fir in coast and interior of British Columbia. Forest Ecol. Manage. 165, 285–293.
Weis, E., Berry, J.A., 1987. Quantum efficiency of Photosystem II in relation to 'energy'-dependent quenching of chlorophyll fluorescence. Biochim. Biophys. Acta 894, 198–208.
Wilson, K.B., Baldocchi, D.D., Hanson, P.J., 2000. Spatial and seasonal variability of photosynthetic parameters and their relationship to leaf nitrogen in a deciduous forest. Tree Physiol. 20, 565–578.
Wilson, K.B., Baldocchi, D.D., Hanson, P.J., 2001. Leaf age affects the seasonal pattern of photosynthetic capacity and net ecosystem exchange of carbon in a deciduous forest. Plant Cell Environ. 24, 571–583.
Woebbecke, D.M., Meyer, G.E., Von Bargen, K., Mortensen, D.A., 1995. Color indices for weed identification under various soil, residue and lightening conditions. Trans. Am. Soc. Agric. Eng. 38, 259–269.
Wright, I.J., Reich, P.B., Westoby, M., Ackerly, D.D., Baruch, Z., Bongers, F., Cavender-Bares, J., Chapin, T., Cornelissen, J.H.C., Diemer, M., Flexas, J., Garnier, E., Groom, P.K., Gulias, J., Hikosaka, K., Lamont, B.B., Lee, T., Lee, W., Lusk, C., Midgley, J.J., Navas, M.-L., Niinemets, Ü., Oleksyn, J., Osada, N., Poorter, H., Poot, P., Prior, L., Pyankov, V.I., Roumet, C., Thomas, S.C., Tjoelker, M.G., Veneklaas, E.J., Villar, R., 2004. The worldwide leaf economics spectrum. Nature 428, 821–827.